Thermal Lens Spectrometry: Theory and Applications

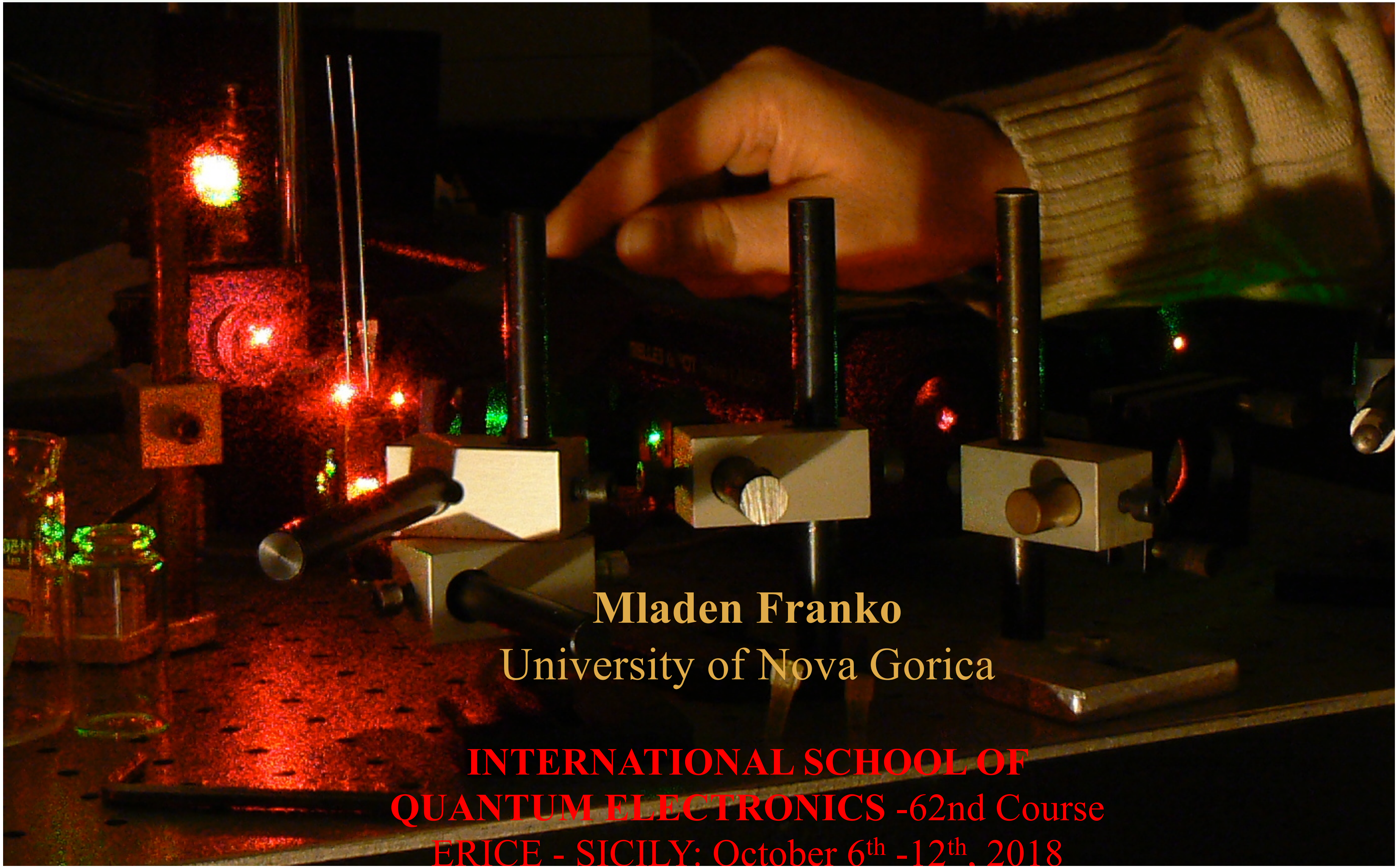

Mladen Franko
University of Nova Gorica

INTERNATIONAL SCHOOL OF QUANTUM ELECTRONICS -62nd Course
ERICE - SICILY: October 6^{th} -12^{th}, 2018

Outline

1. Basics of TLS spectrometry and comparison to UV-Vis spectrometry
2. Principles of collimated PB and multi-pass TLS instruments
3. Novel tunable TLS spectrometers
4. Limitations of multi-pass instruments
    1. Linearity range
    2. Effects of blank
5. Applications

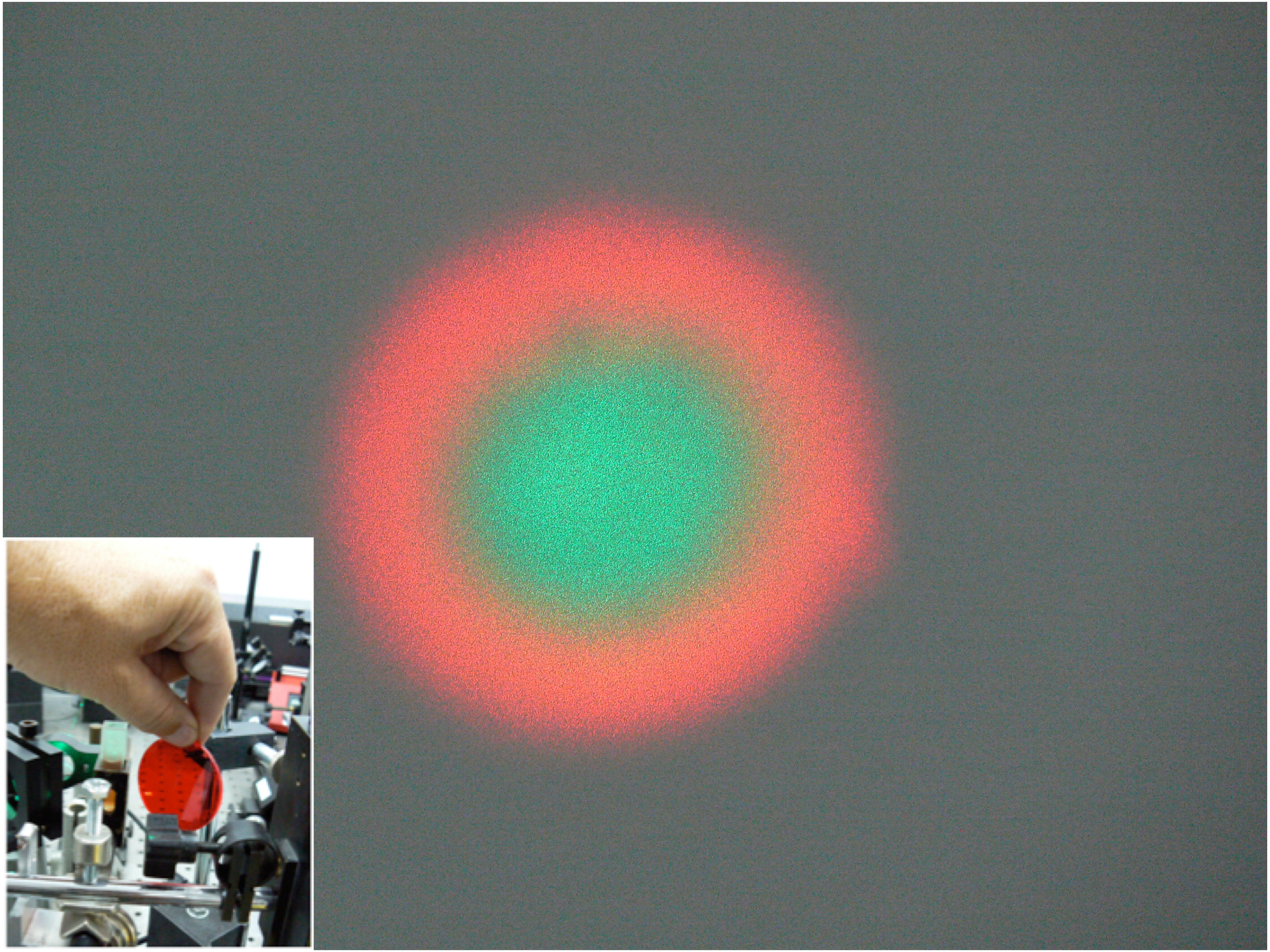

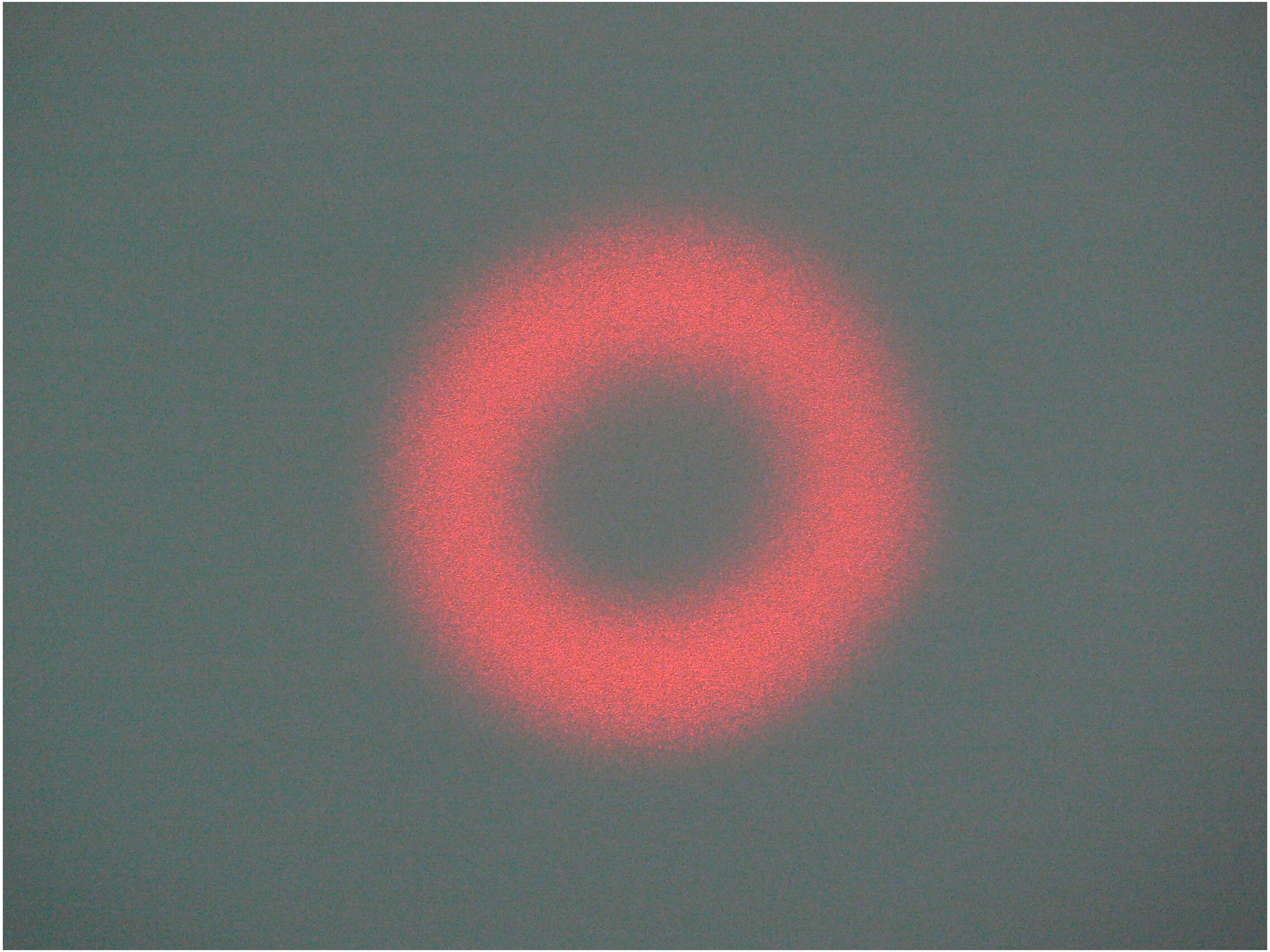

Basics of thermal lens effect

- During non-radiative relaxation of excited species temperature in the sample increases (10^{-4} - 10^{-3} K)
- a temperature gradient is generated with maximum temperature at the axis of the excitation beam
- the resulting refractive index gradient acts as a lens (mostly: $dn/dT < 0$, diverging lens)
- laser beam is defocused (single beam or pump/probe configuration)
- beam radius and its intensity at the beam axis changes
- relative change in the beam intensity is proportional to the absorbed power of the excitation beam.

TLS effect is time dependent - signal forms

Pulsed excitation

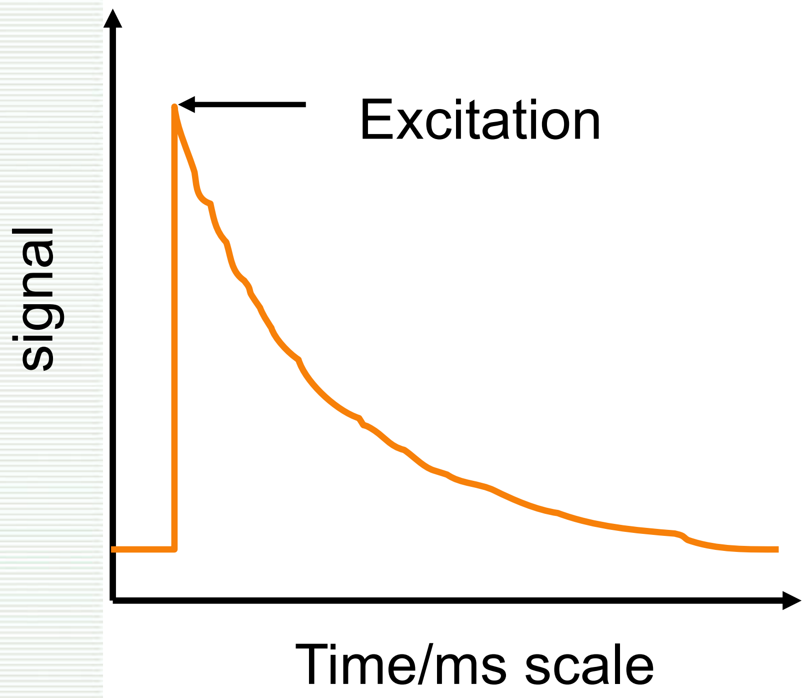

CW excitation

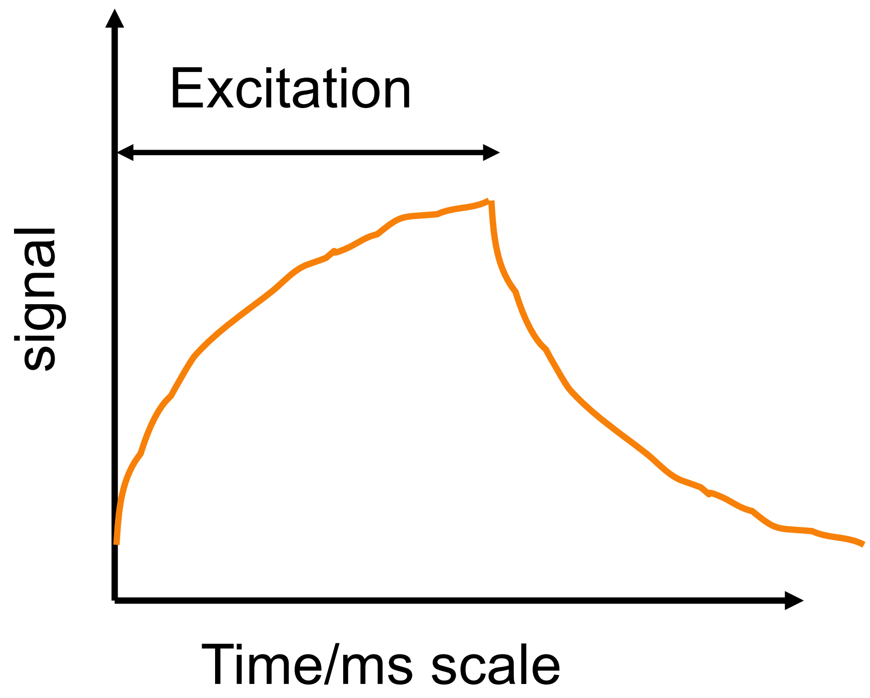

Parameters affecting TL signal

- **Absorbance** (concentration), **Power** of excitation beam (I_0, usually denoted as P)

$$I = I_0 10^{-A}$$

$$I = I_0 e^{-2.303A}$$

$$e^A = 1 + \frac{A}{1!} + \frac{A^2}{2!} + \frac{A^3}{3!} + \ldots$$

$$\frac{I}{I_0} = 1 - \frac{2.303A}{1!} + \frac{2.303^2 A^2}{2!} - \frac{2.303^3 A^3}{3!} + \ldots$$

$$\frac{I - I_0}{I_0} = -\frac{2.303A}{1!} + \frac{2.303^2 A^2}{2!} - \frac{2.303^3 A^3}{3!} + \ldots$$

Absorbed power is linearly proportional to absorbance only for small A (< 0.1) !!!

Parameters affecting TL signal II.

- Optothermal parameters of sample/medium
  - **Thermal conductivity (*k*), temperature coefficient of refractive index (*dn/dT*)**
- Probe beam wavelength (λ)

$$\Theta = -\frac{2.303PA(\frac{dn}{dT})}{\lambda k}$$

- Beam geometry factors: probe and pump beam radii (w_p, w_e), position of sample (z)

$$m = \left(\frac{w_p}{w_e}\right)^2, V = \frac{Z_1}{Z_c} + \frac{Z_c}{Z_2}\left[1 + \left(\frac{Z_1}{Z_c}\right)^2\right], \quad Z_c = \frac{\pi w_{0p}{}^2}{\lambda}$$

TLS experiment

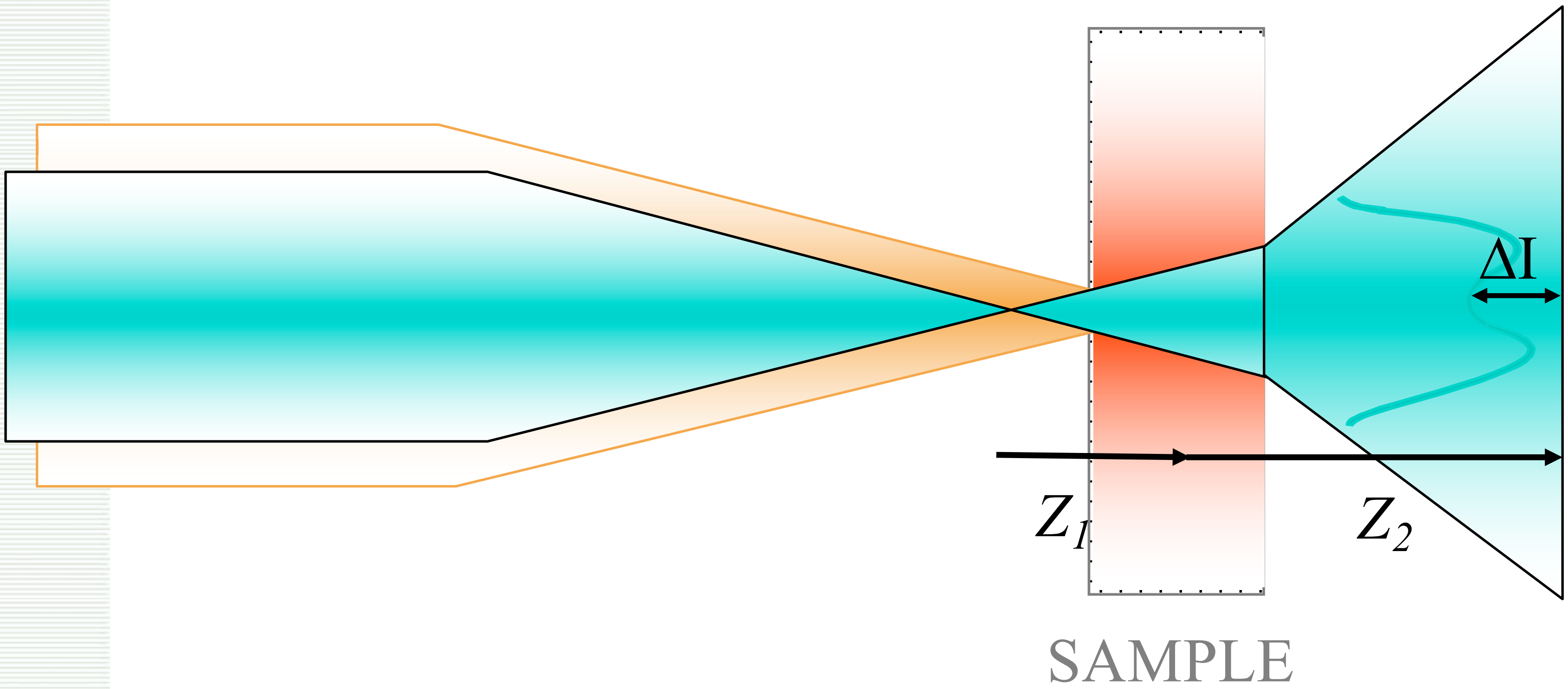

- Bimodal behavior: $\pm Z_1$

$$V = \frac{Z_1}{Z_c} + \frac{Z_c}{Z_2}\left[1 + \left(\frac{Z_1}{Z_c}\right)^2\right]$$

Mathematical description of TLS effect/signal

TL causes a phase shift in propagation of probe beam

$$\Delta\Phi(r,z,t) = -\frac{\Theta}{t_c(z)}\int_0^t \frac{dt'}{1+2t'/t_c(z)}\left[1-\exp\left(-\frac{2r^2}{\omega_e^2(z)(1+2t'/t_c(z))}\right)\right]$$

$$I(t) = $$

$$= I(0)\left\{\left[1-\frac{\theta}{2}\arctan\left(\frac{2mV}{[(1+2m)^2+V^2]\left(\frac{t_c}{t}\right)+1+2m+V^2}\right)\right]^2 + \left[\frac{\theta}{4}\ln\left(\frac{[1+2m/(1+t/t_c)]^2+V^2}{(1+2m)^2+V^2}\right)\right]^2\right\}$$

Maximal TL signal

- *arctan* is maximum ($\pi/2$) when argument approaches ∞: highly collimated probe beam

  (no bimodal behavior)

$$S = \frac{\pi\theta}{2} - \frac{\pi^2\theta^2}{16}$$

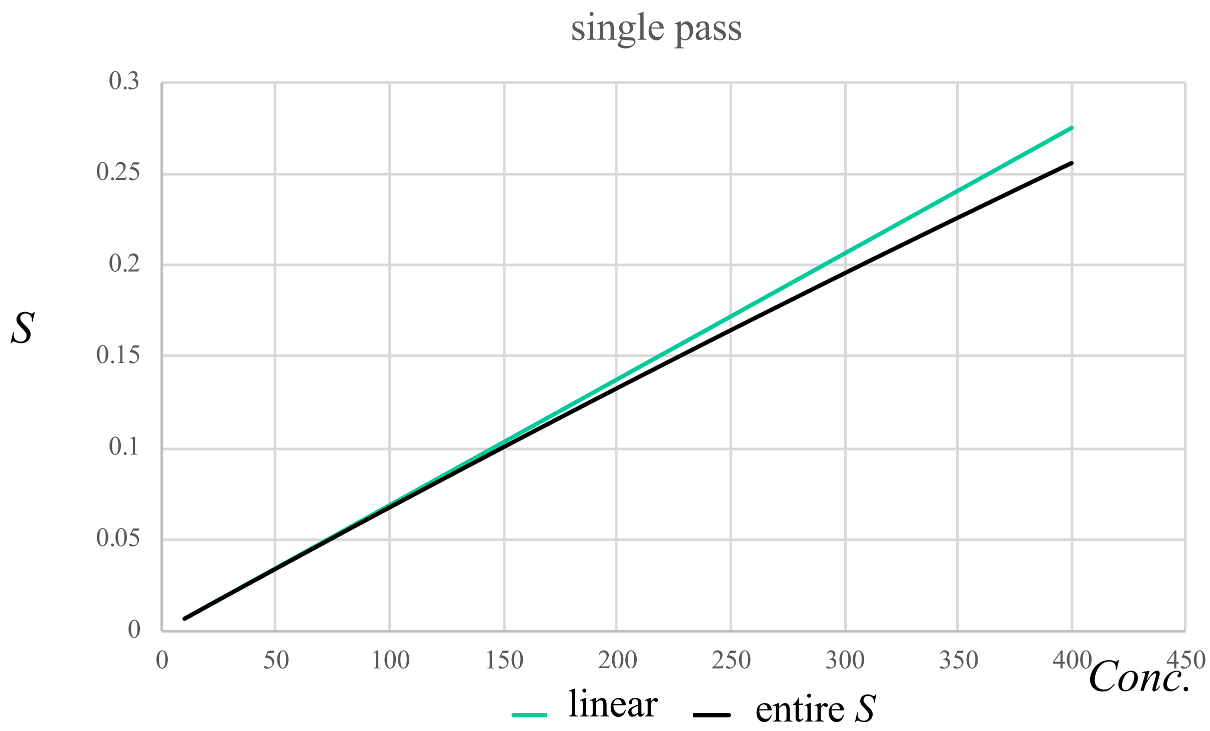

Blank subtraction by differential TLS measurements

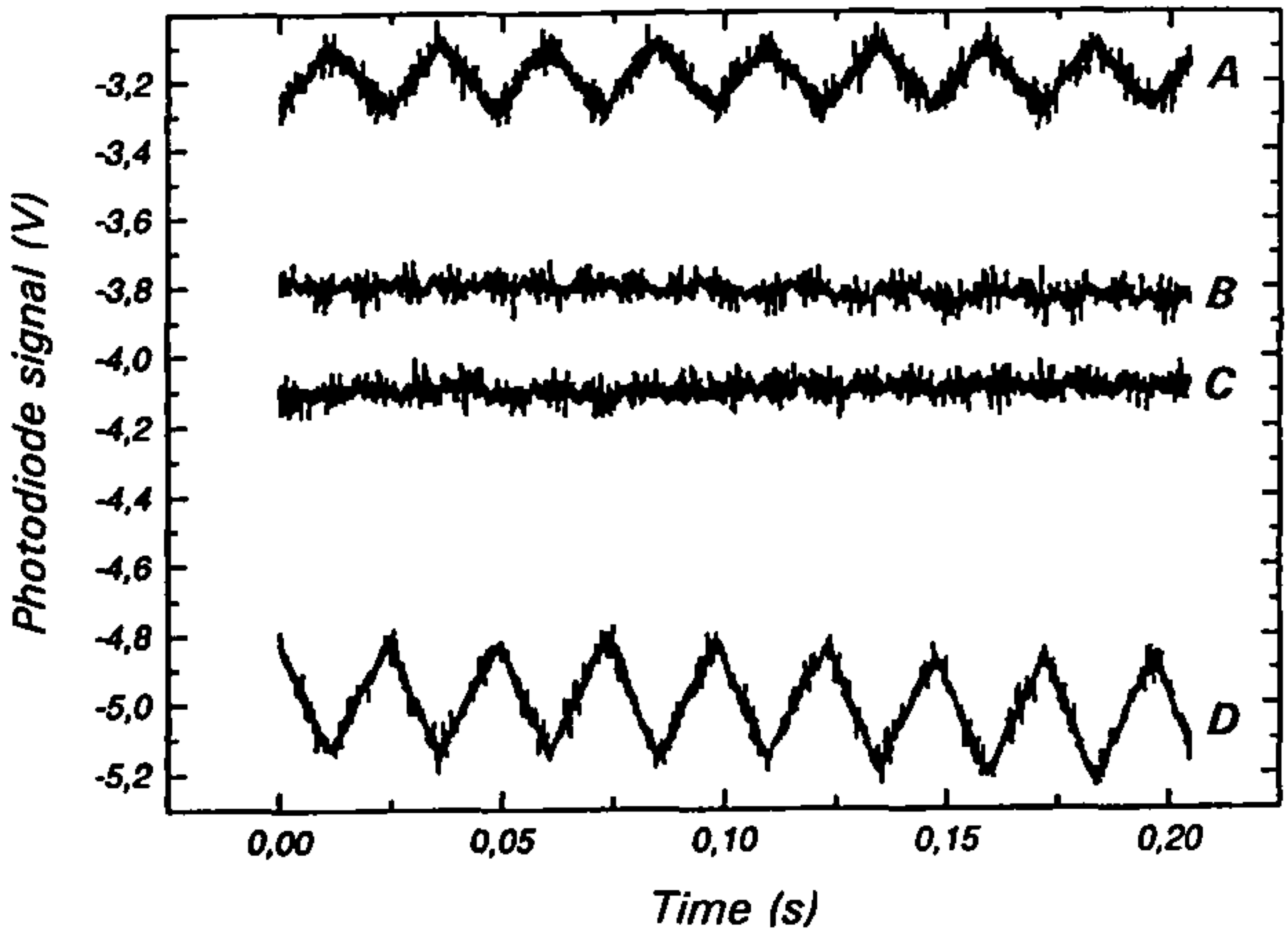

E - Enhancement factor in TLS

For spectrophotometry: $\frac{I_0 - I}{I_0} = \frac{2.303A}{1!}$ therefore:

for m = 1 and $z_1 = z_c\sqrt{3}$: and for max. signal:

$$E = -\frac{P\left(\frac{dn}{dT}\right)0.534}{\lambda k}$$

$$E_{coll} = -\frac{P(\frac{dn}{dT})\pi}{2\lambda k}$$

Solvent	$-dn/dT$ / 10^{-4}K^{-1}	k / W m^{-1}K^{-1}	E /10^{-3} W^{-1}
H_2O	0.91	0.607	0.12 (0.35)
CCl_4	5.9	0.103	4.74 (13.9)
acetone	5.42	0.190	2.36 (6.94)

E is calculated for $\lambda = 632.8$ nm (E_{coll} is given in parentheses)

Adjustable beam size/position TLM

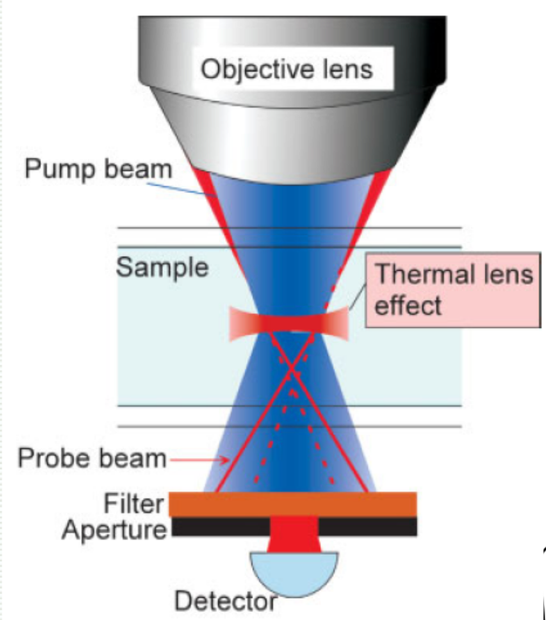

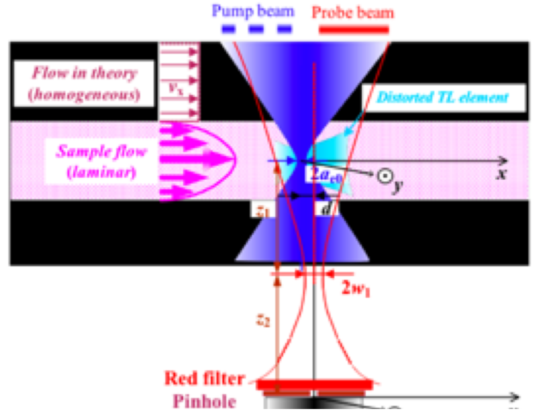

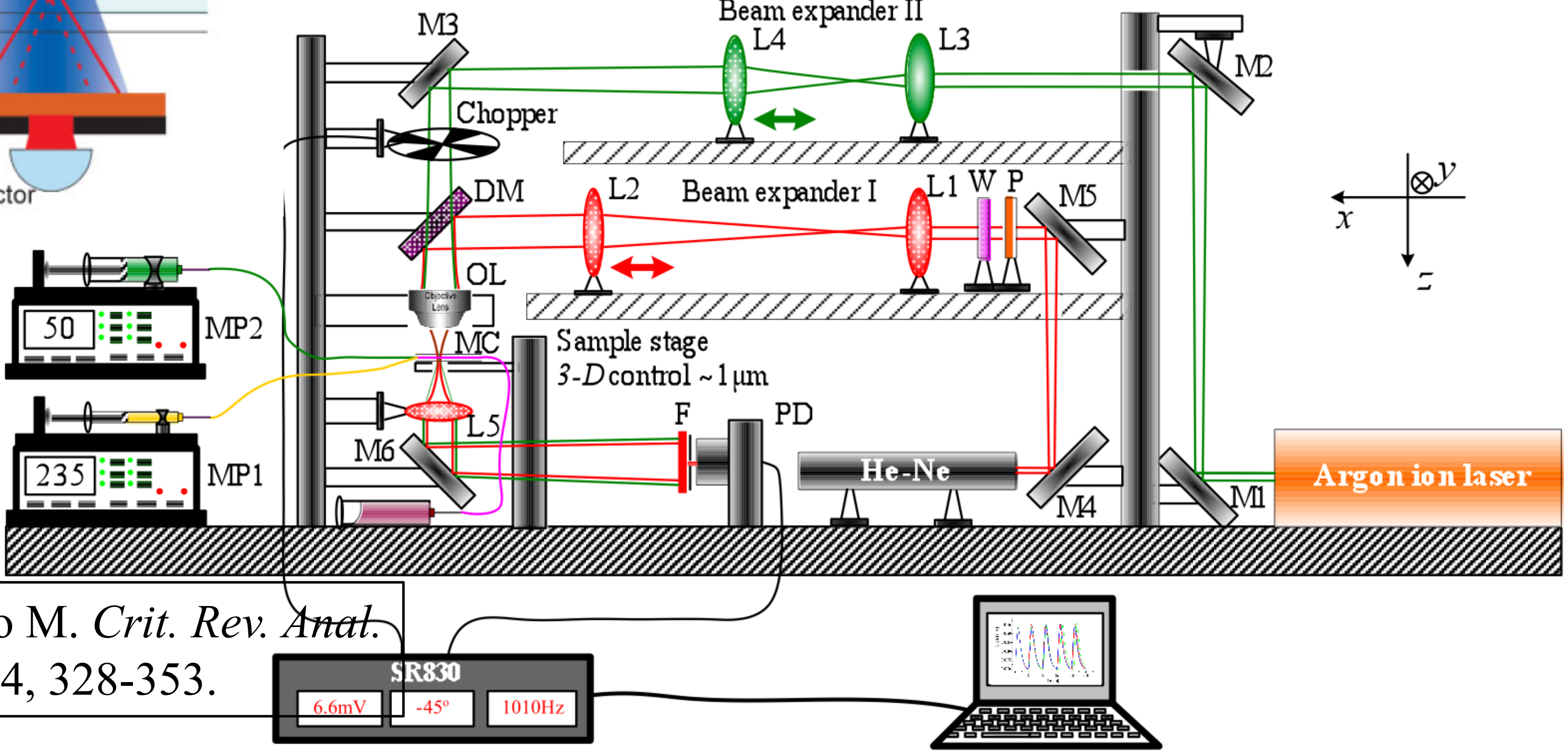

Liu M., Franko M. *Crit. Rev. Anal. Chem.* **44**, 2014, 328-353.

TLM detection in microfluidic systems

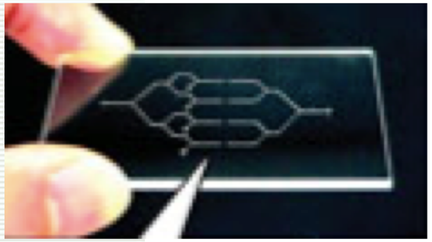

Microchip

TLM

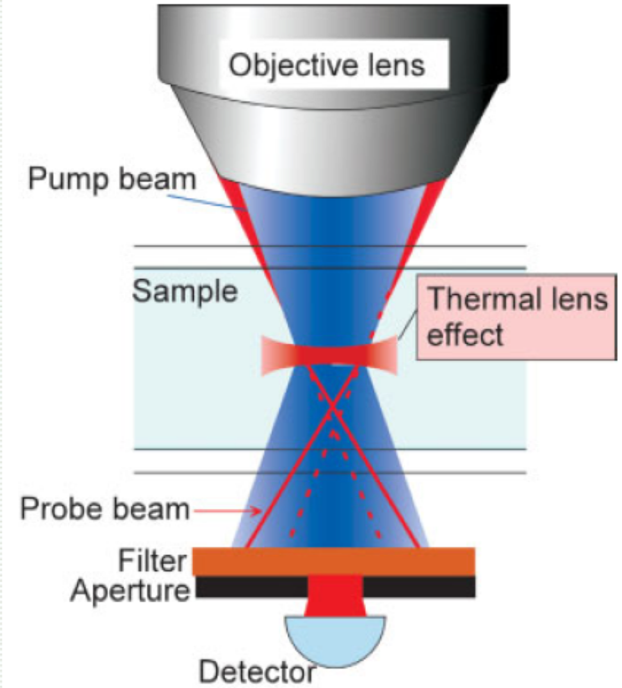

Microchannel-based immunoassay

assay time of s-IgA
24 h → 20 min

channel size

$$t_m = L_m^2 / D_m$$

$$\sigma_m = S_m / V_m \propto 1 / L_m$$

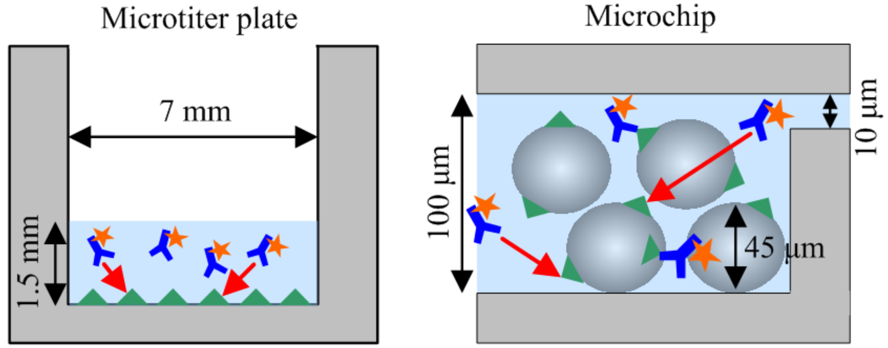

MUOs

Microunit operations

CFCP

Continuous flow chemical processing

Trace cobalt (LOD 0.13 zmol)

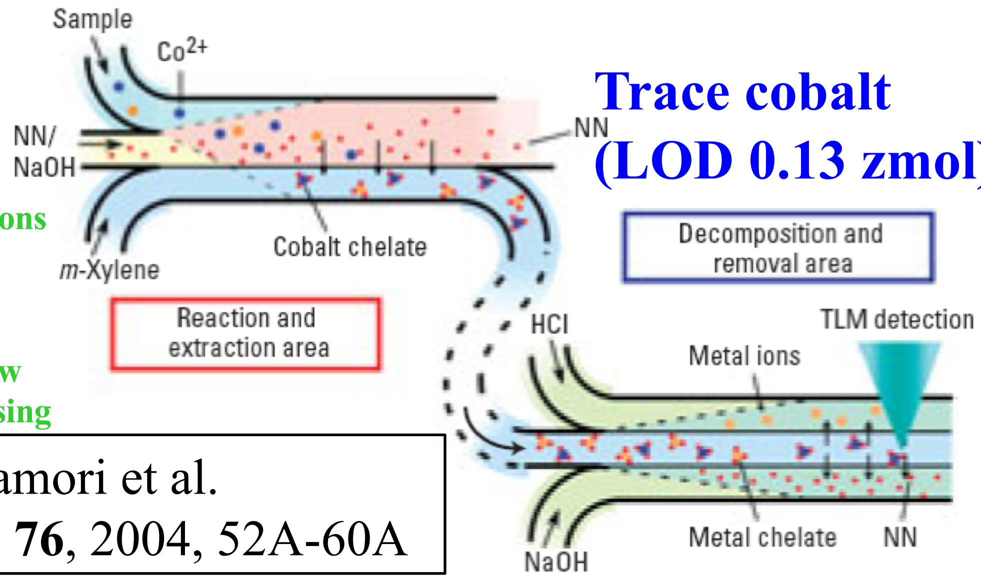

From: T. Kitamori et al.
Anal. Chem., **76**, 2004, 52A-60A

Efficiency of TLM for different sample thicknesses

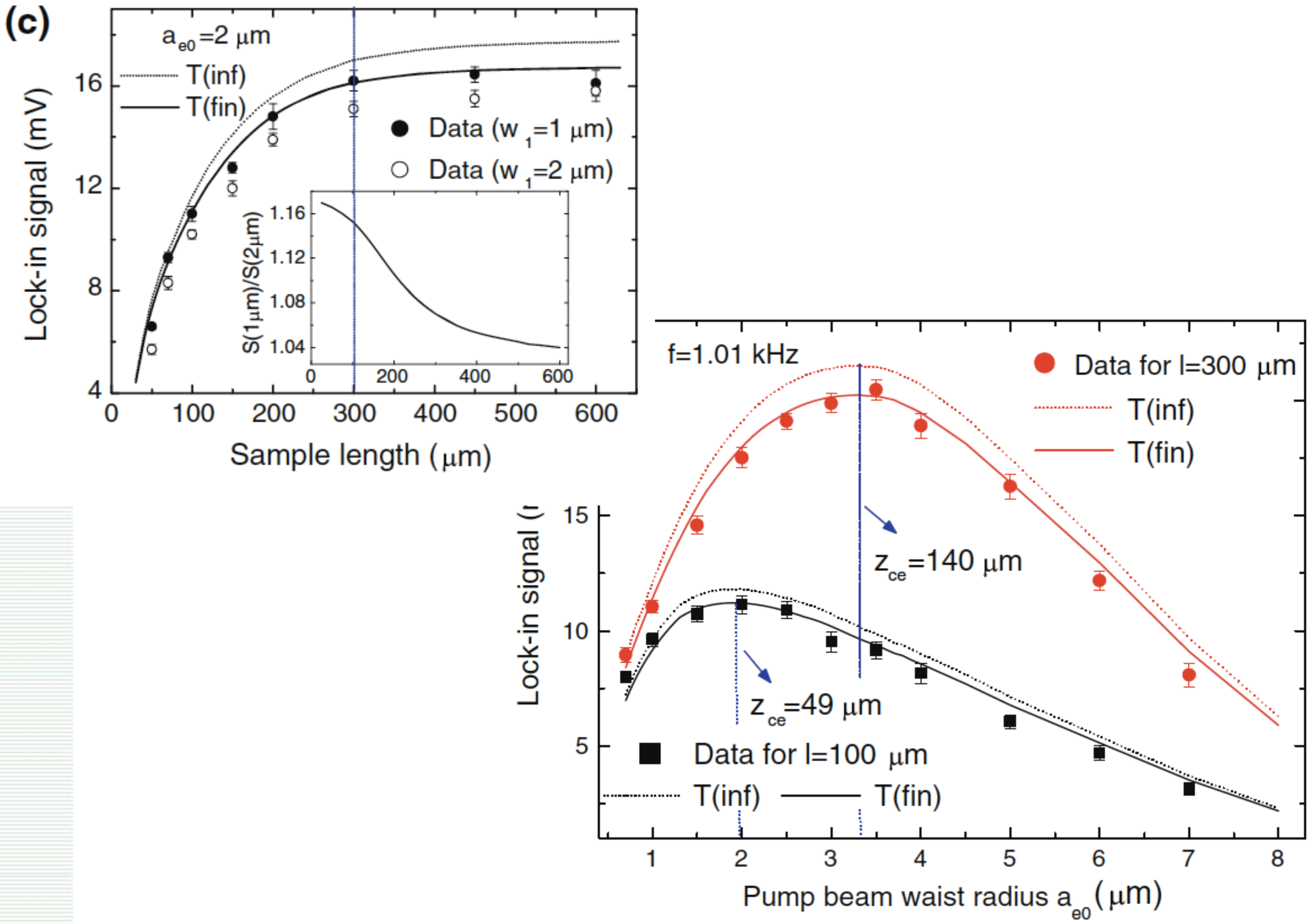

Multi-pass TLS instrument

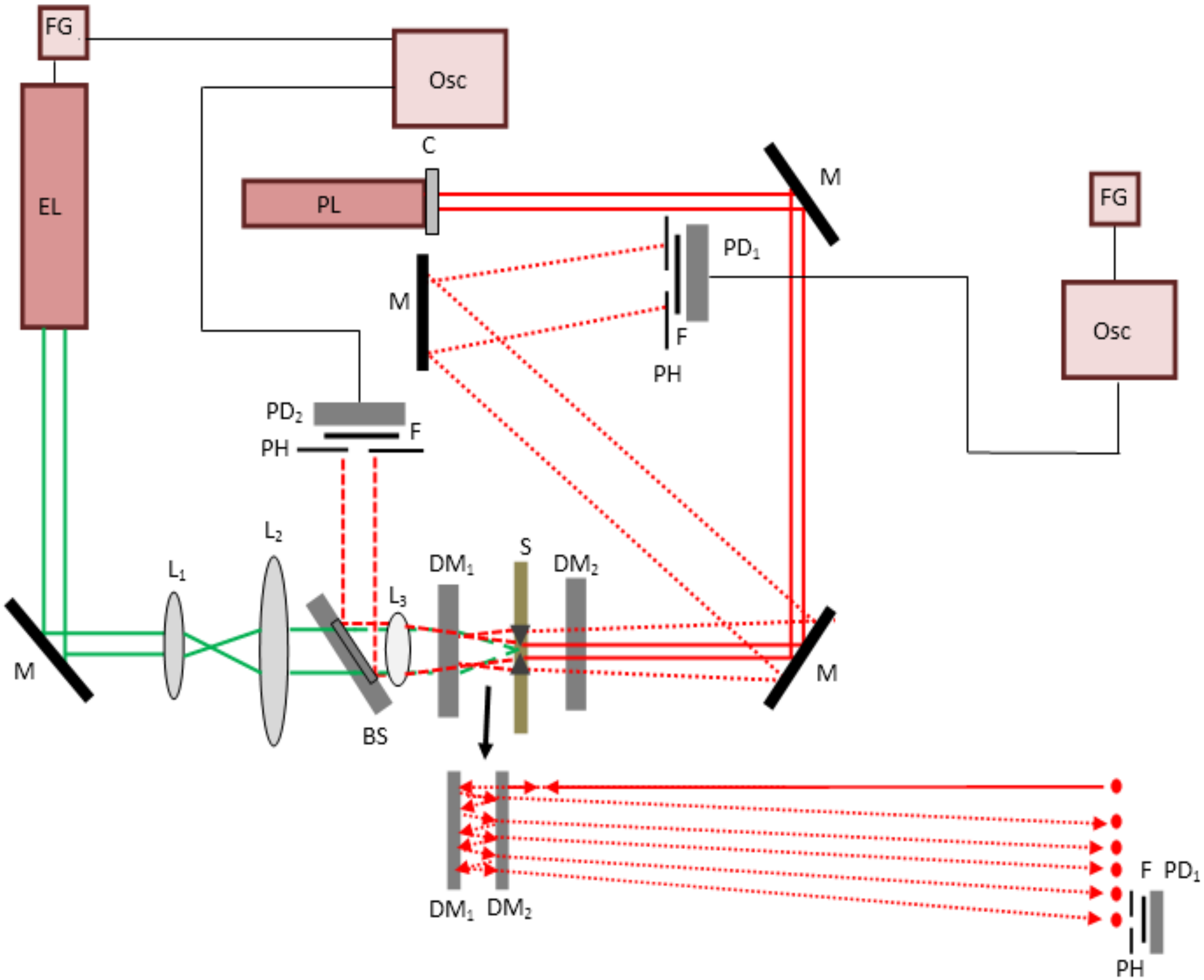

Signal in multi-pass TLS measurements

$$\Delta\Phi(r,z,t) = -n\frac{\Theta}{t_c(z)}\int_0^t \frac{dt'}{1+2t'/t_c(z)}\left[1-\exp\left(-\frac{2r^2}{\omega_e^{\,2}(z)(1+2t'/t_c(z))}\right)\right]$$

$$S = \frac{n\pi\theta}{2} - \frac{n^2\pi^2\theta^2}{16}$$

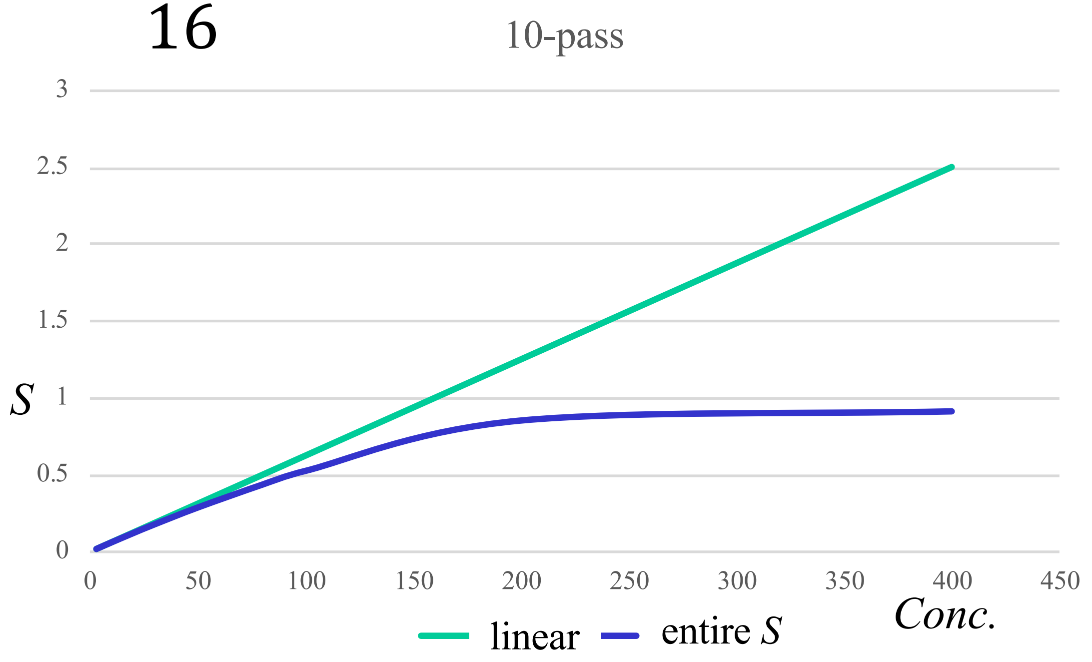

Milti-pass TLS measurements of Fe(II)-1,10 phenanthroline

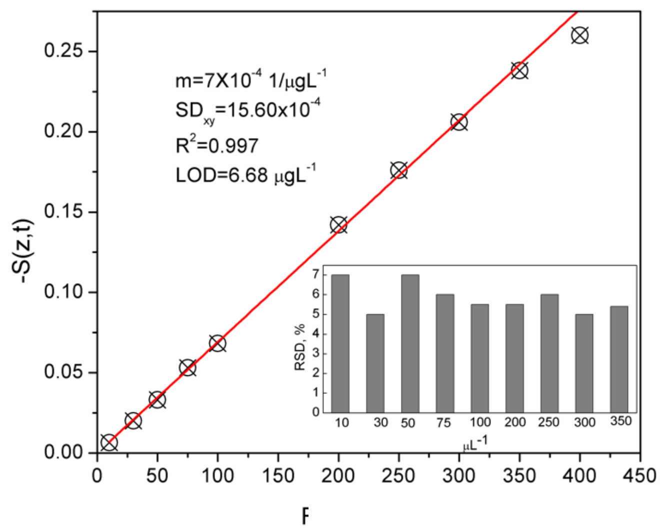

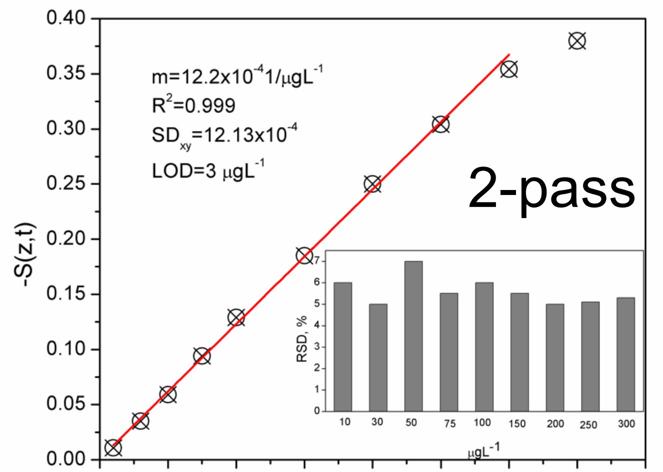

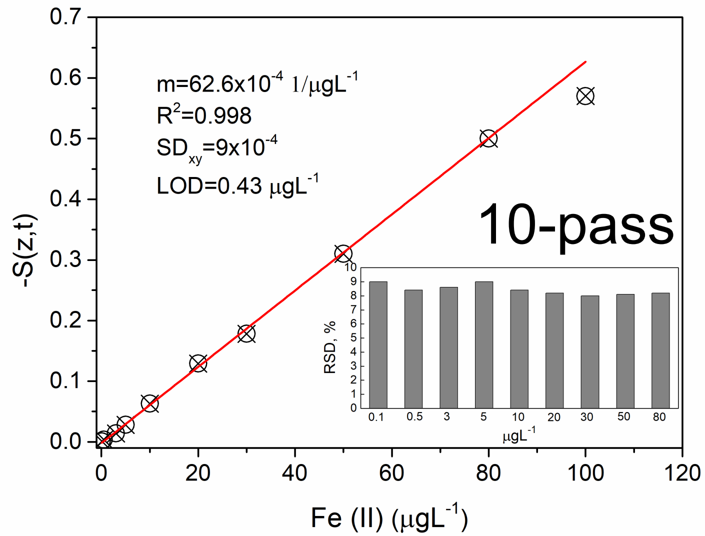

P=20 mW,
@ 532.8 nm

Blank effects

$$\theta = \theta_s + \theta_b$$

Leads to a mixed term in TLS signal: $-\dfrac{n^2\pi^2\theta_s\theta_b}{8}$

which can not be subtracted by subtracting the blank signal

$$S_b = \frac{n\pi\theta_b}{2} - \frac{n^2\pi^2\theta_b^2}{16}$$

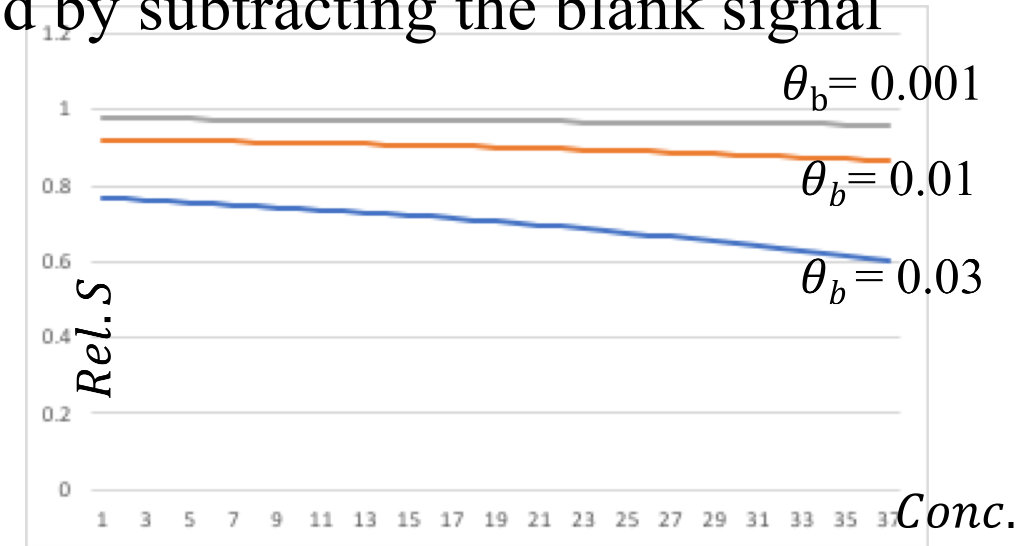

This leads to 25-40% errors in 10-pass configuration

for large θ. e.g. $\theta_b = 0.03$

for $\theta_b = 0.01$ error is between 8 and 15% ($A_{max.} = 0.05$/cm)

the effect increases with increasing concentration of analyte.

It can be neglected for single and dual pass configurations.

TLS - advantages

- High sensitivity
    - signal proportional to excitation laser power
    - absorbances as low as 10^{-7} can be measured
- Enables On-line detection
    - fast response of TLS signal (on μs to ms time scale)
- Capability of measuring small samples
    - sub-pL volumes can be probed
    - detection in microfluidic systems

TLS – drawbacks and solutions

- Sensitivity still needs improvement
  - Higher laser power? (photo-labile compounds)
  - Modify solvents
- Limited availability of laser sources
  - Coloring reactions, indirect detection
- Poor selectivity
  - Single wavelength measurements
  - Coupling to separation techniques (HPLC, IC, CE)
- Photodegradation
  - Measure in flowing systems

Tunable Multi-pass TL spectrometer

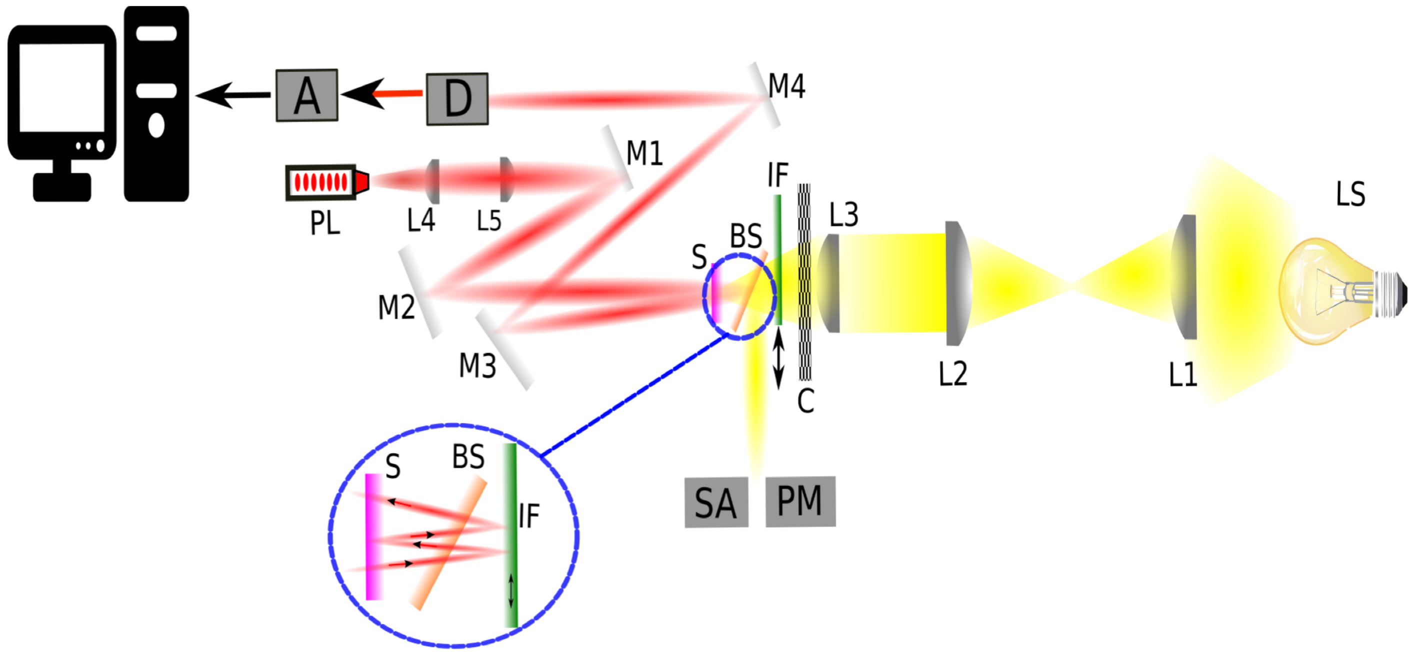

P_e = 7 - 17 mW, 10 nm FWHM, 4-pass configuration

Recording TLS spectra with a multi-pass TL spectrometer

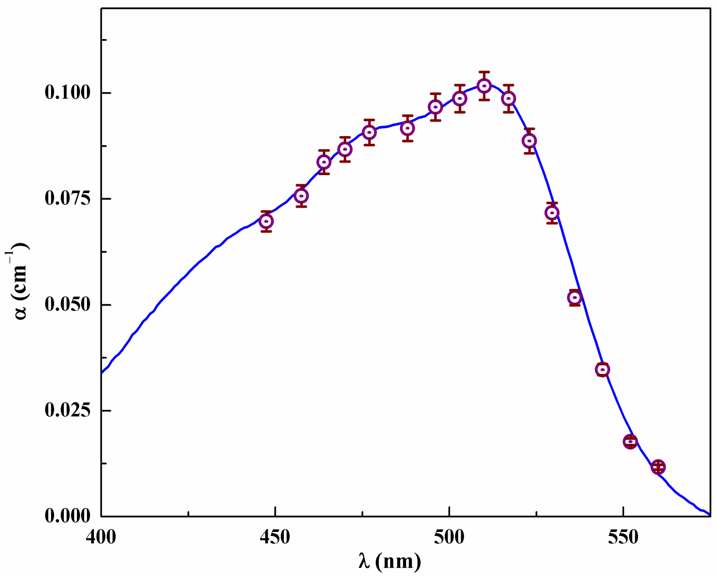

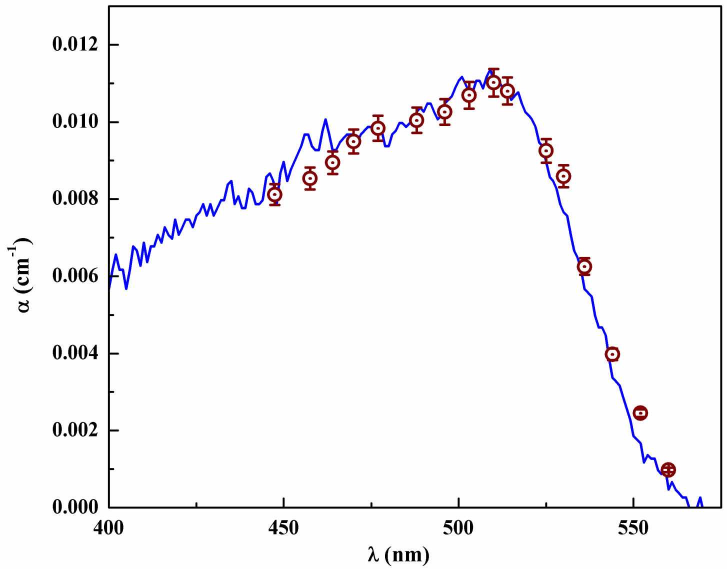

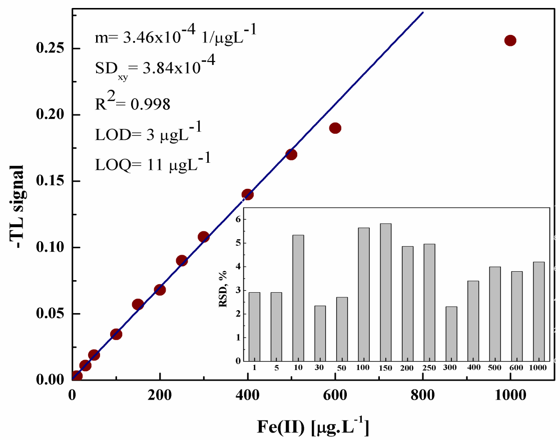

TLS spectra of luminescent nanogold materials

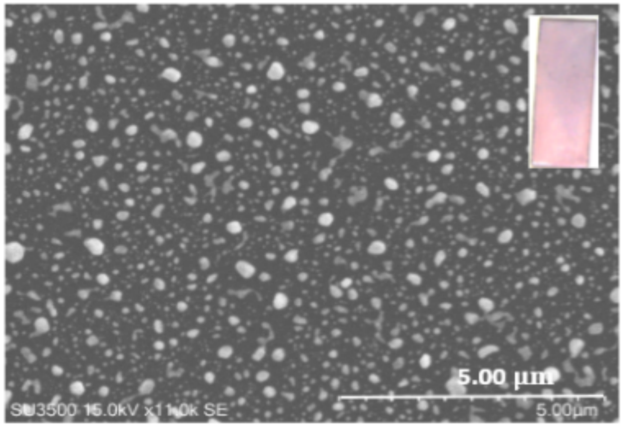

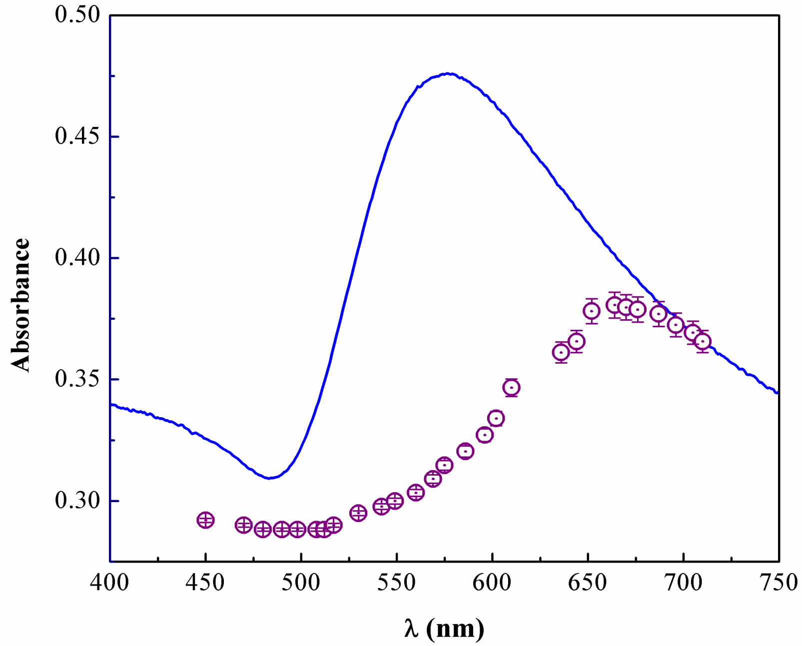

Determination of microcystin by PP2A inhibition assay

Colorimetric reaction catalyzed by PP

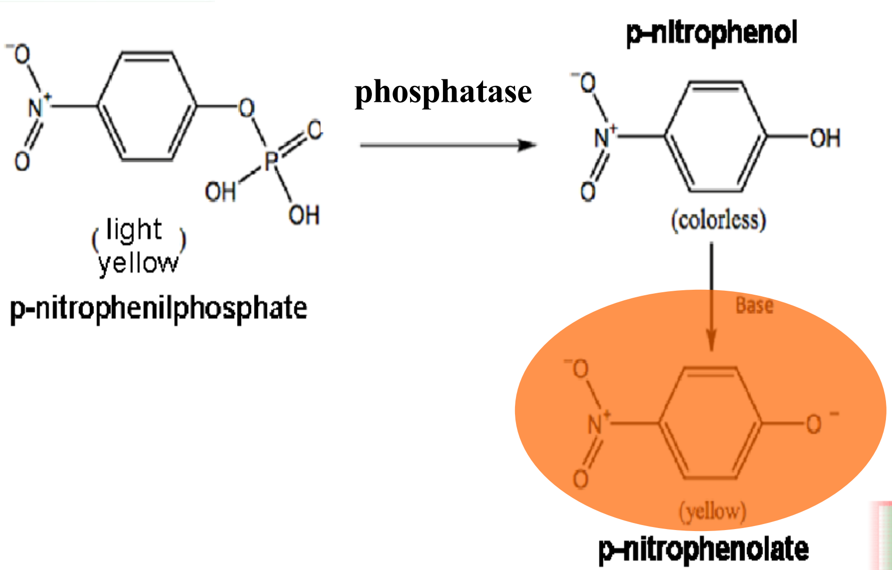

Reaction inhibited by cyanotoxin

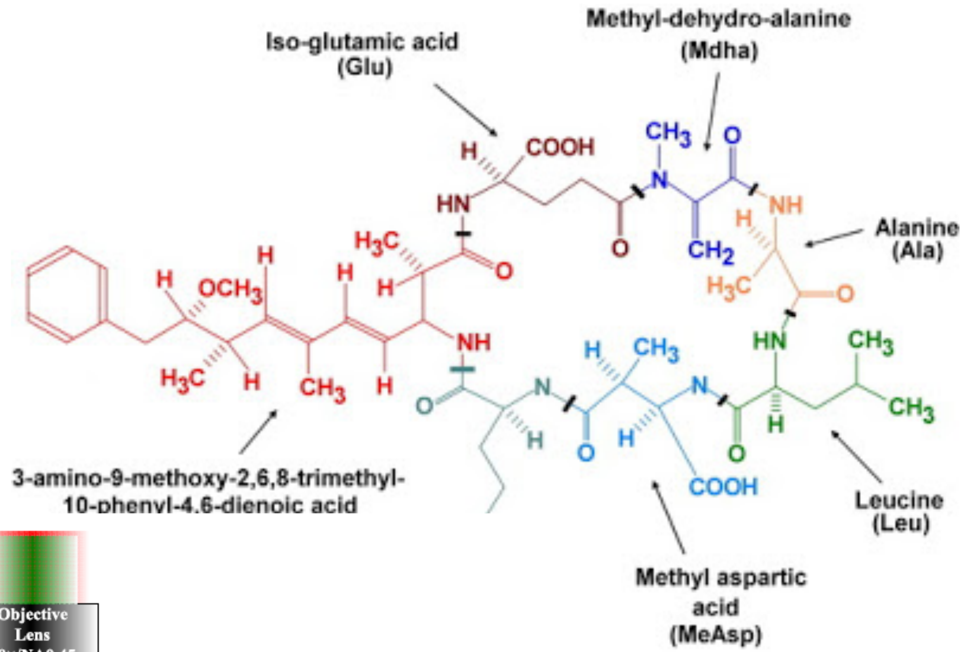

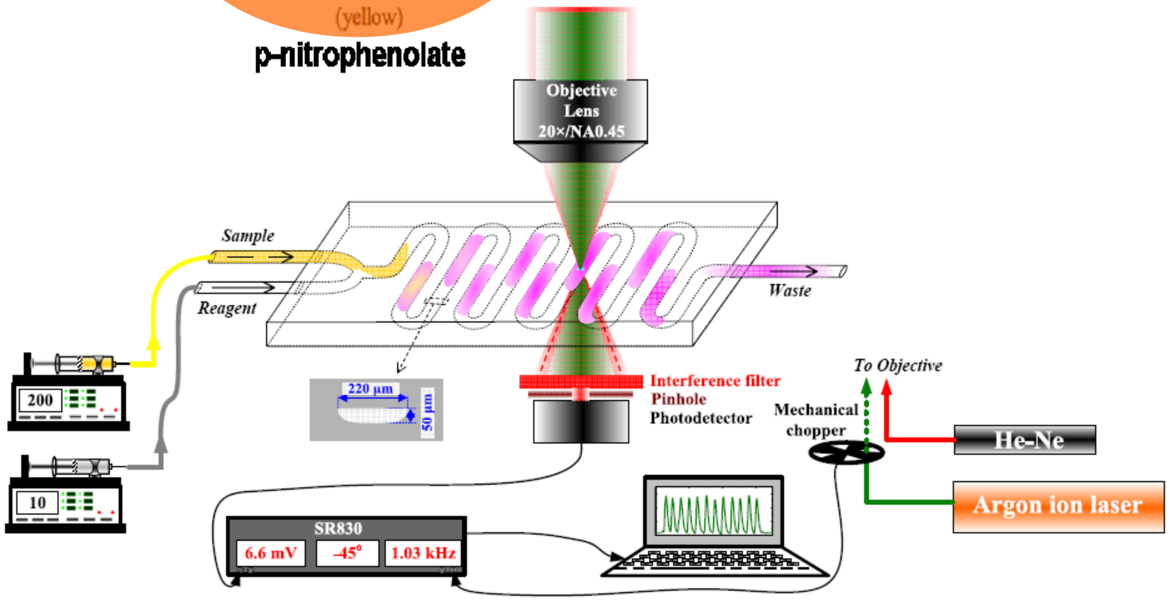

TLM-PP2A inhibition assay

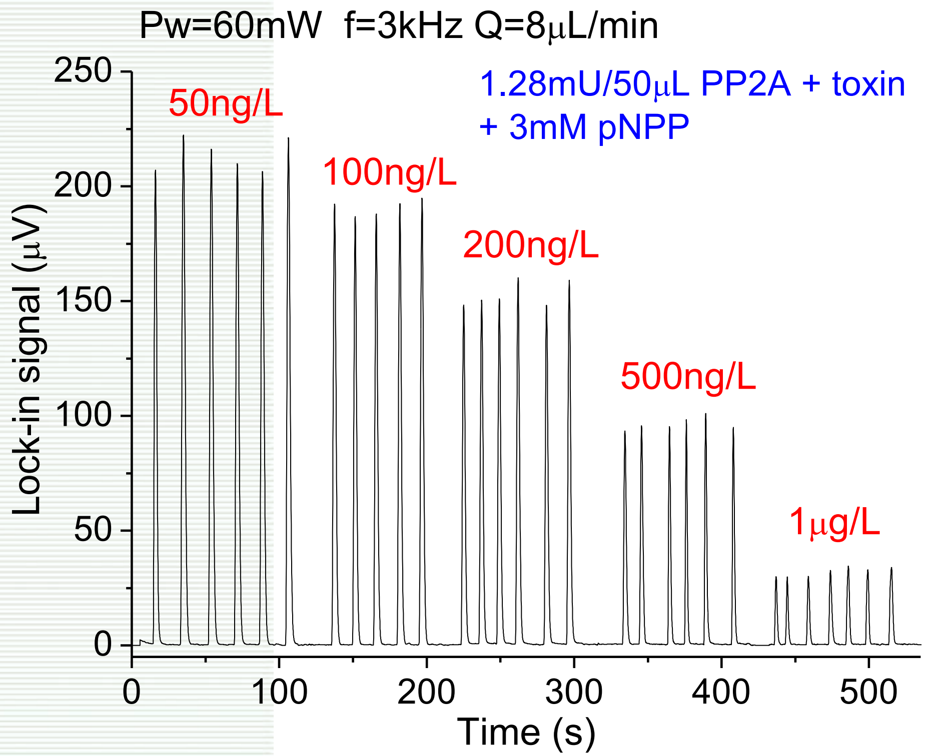

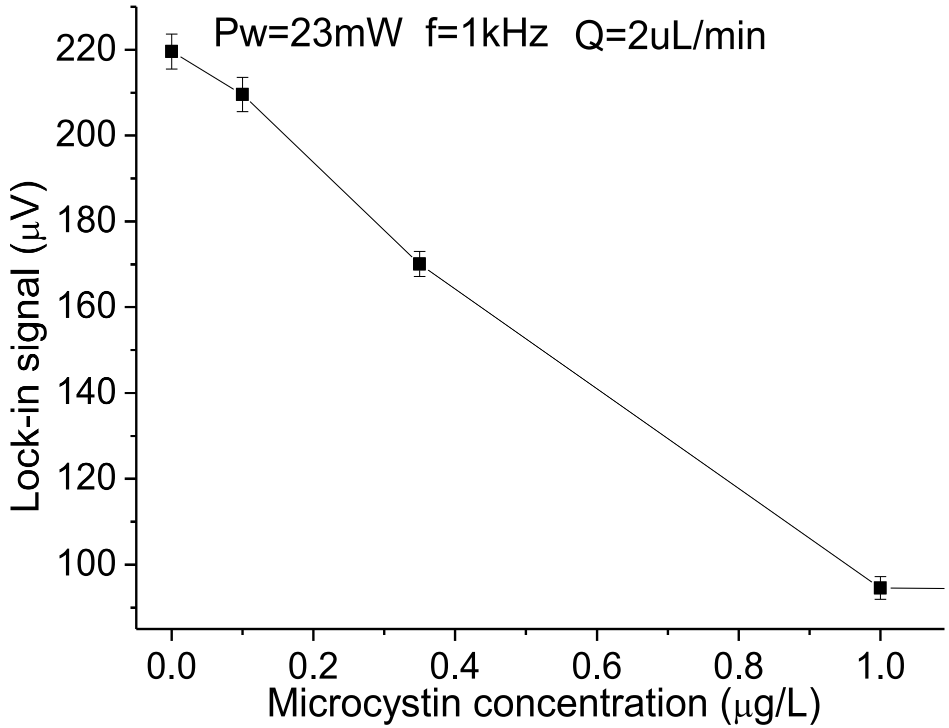

Enzyme consumption: 0.5 μL per injection

Detection limit: ~ 80ng/L

-12 times lower below the WHO limit for drinking water

-8 times faster than batch mode assay

Diffusion in a slag flow

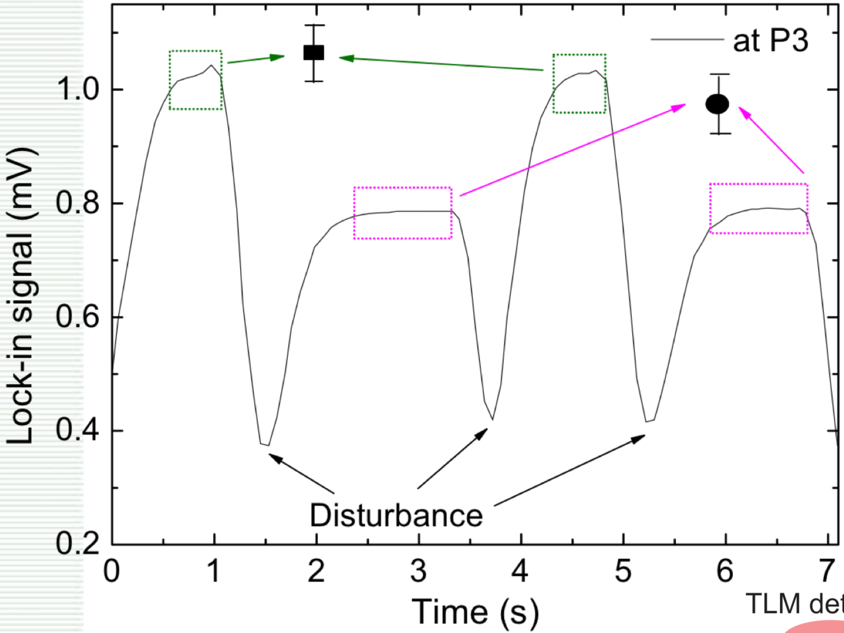

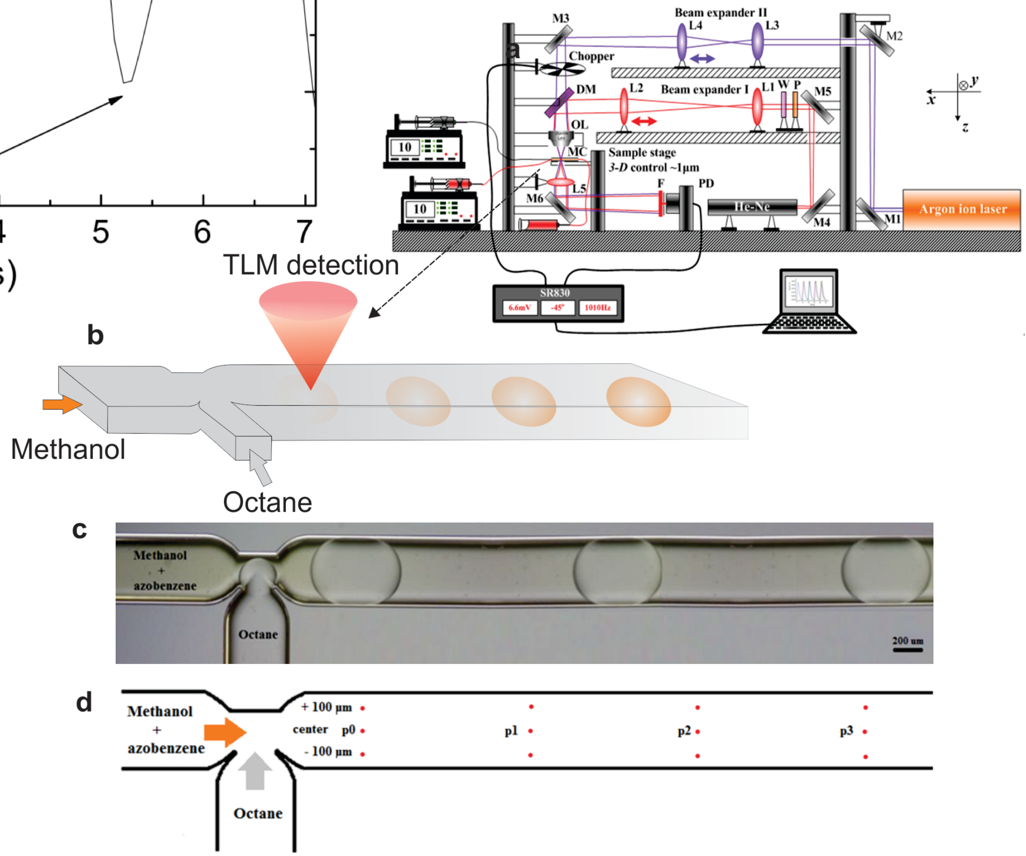

Transport phenomena in multiphase microflows - TLM Based Validation of Models

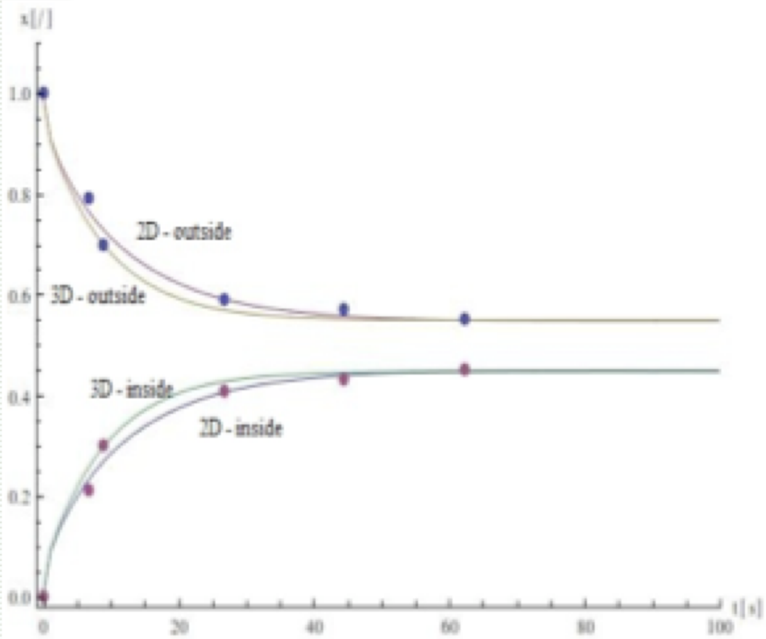

Comparison of 2D and 3D average concentration results outside and inside the slug with experim. measurements.

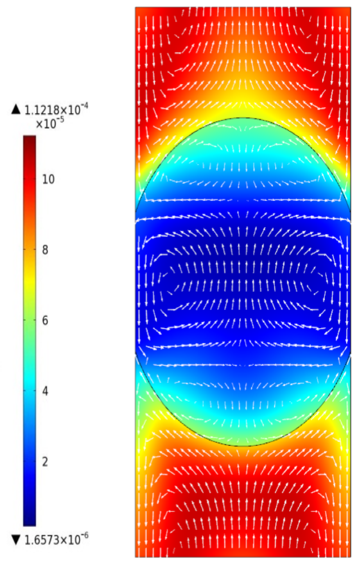

Concentration profile with velocity vectors 2D, τ = 4 s

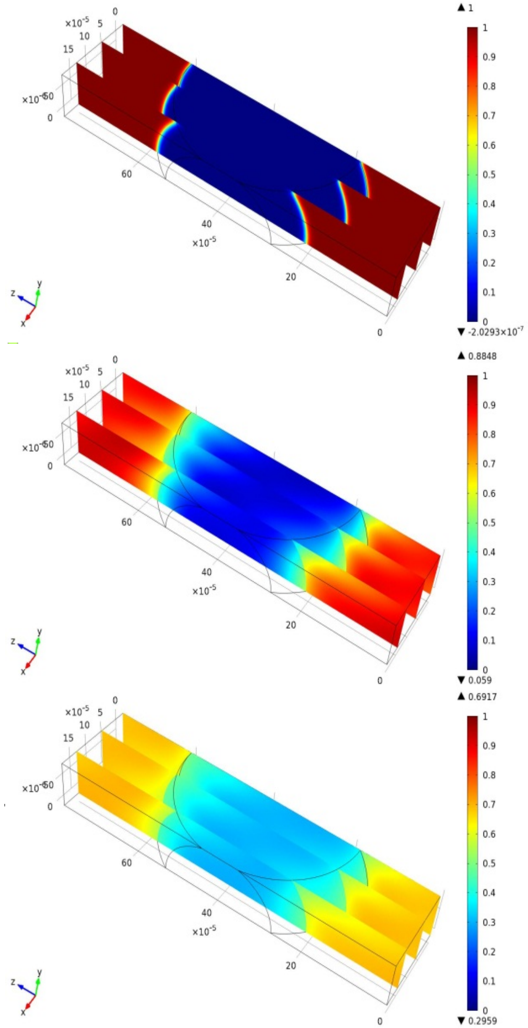

Slug concentration profile over residence time – 0, 4, 12 s.

Lab on a Chip

ROYAL SOCIETY OF CHEMISTRY

PAPER

View Article Online
View Journal

CrossMark

Cite this: DOI: 10.1039/c4lc01460j

Microfluidic droplet-based liquid–liquid extraction: online model validation

Martin Lubej,[a] Uroš Novak,[a] Mingqiang Liu,[b] Mitja Martelanc,[b] Mladen Franko[b] and Igor Plazl*[a]

Detection and utilization of virus-like proteins and pseudovirions

HPV is a cause of cervical cancer.

By using HPV antibodies one can detect HPV.

By using HPV-VLPs one can detect HPV antibodies and past or current infection

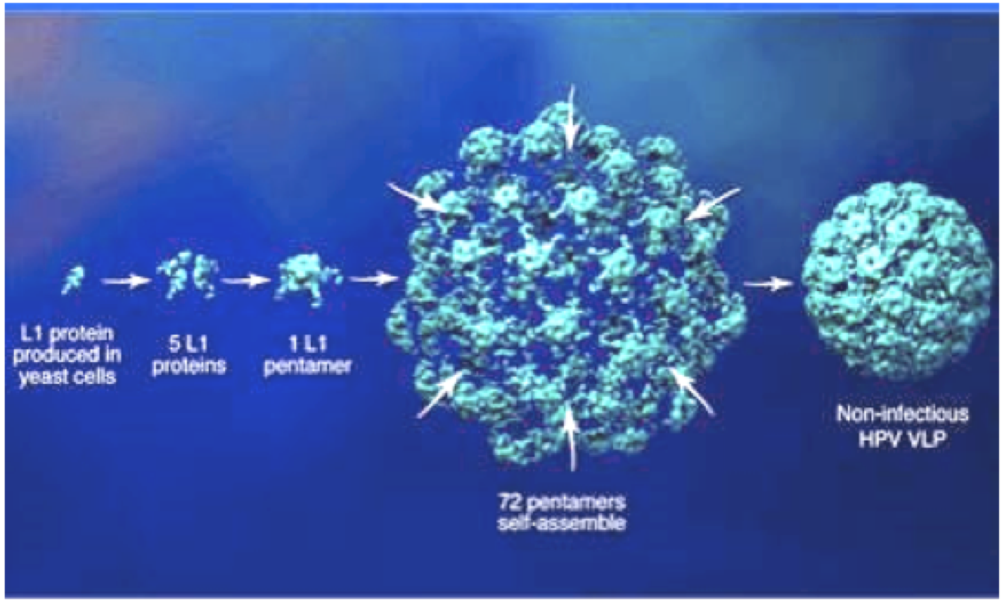

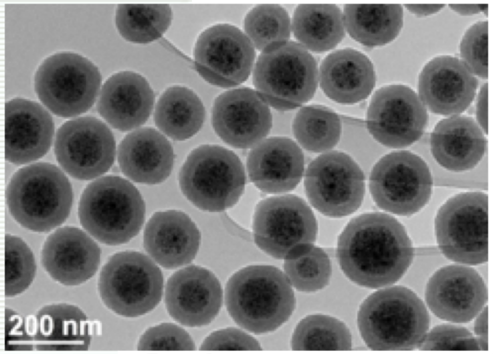

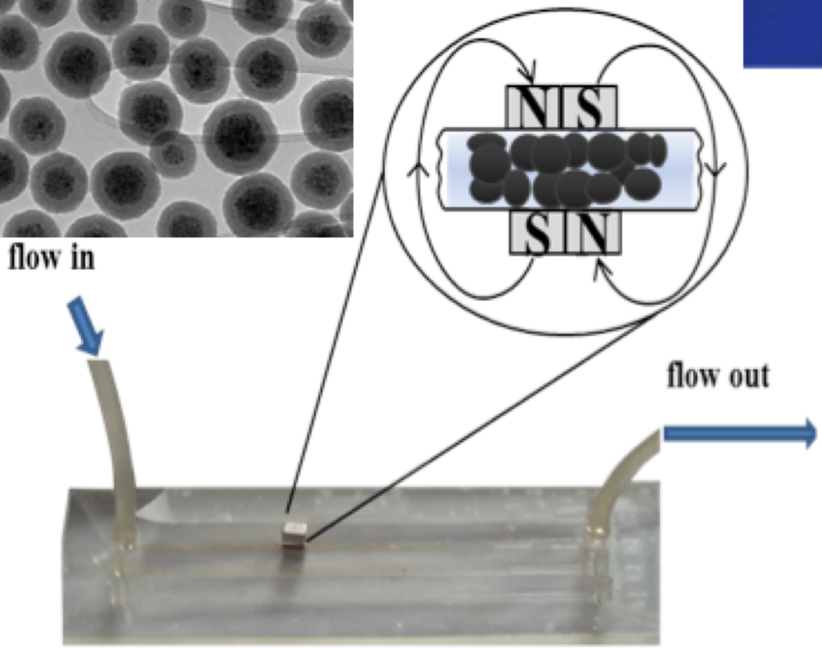

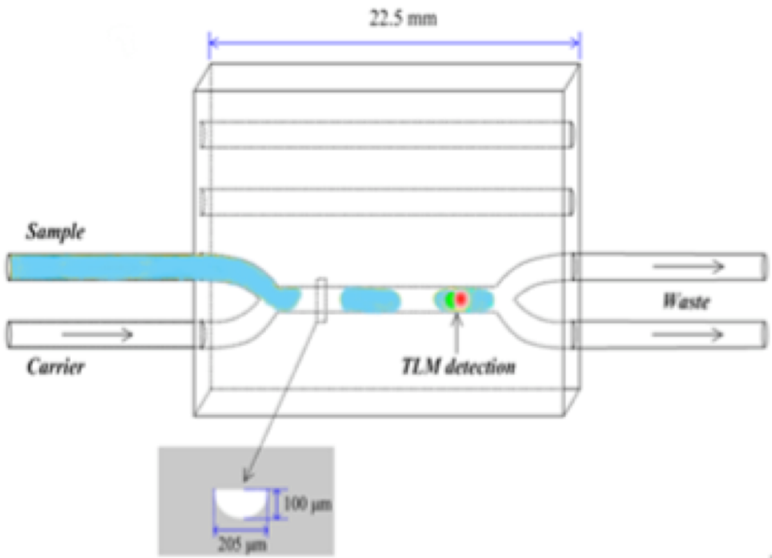

Calibration curves for HPV-16 antibodies

μFIA-TLM on nanobeads: LOD=0.65 ng/mL

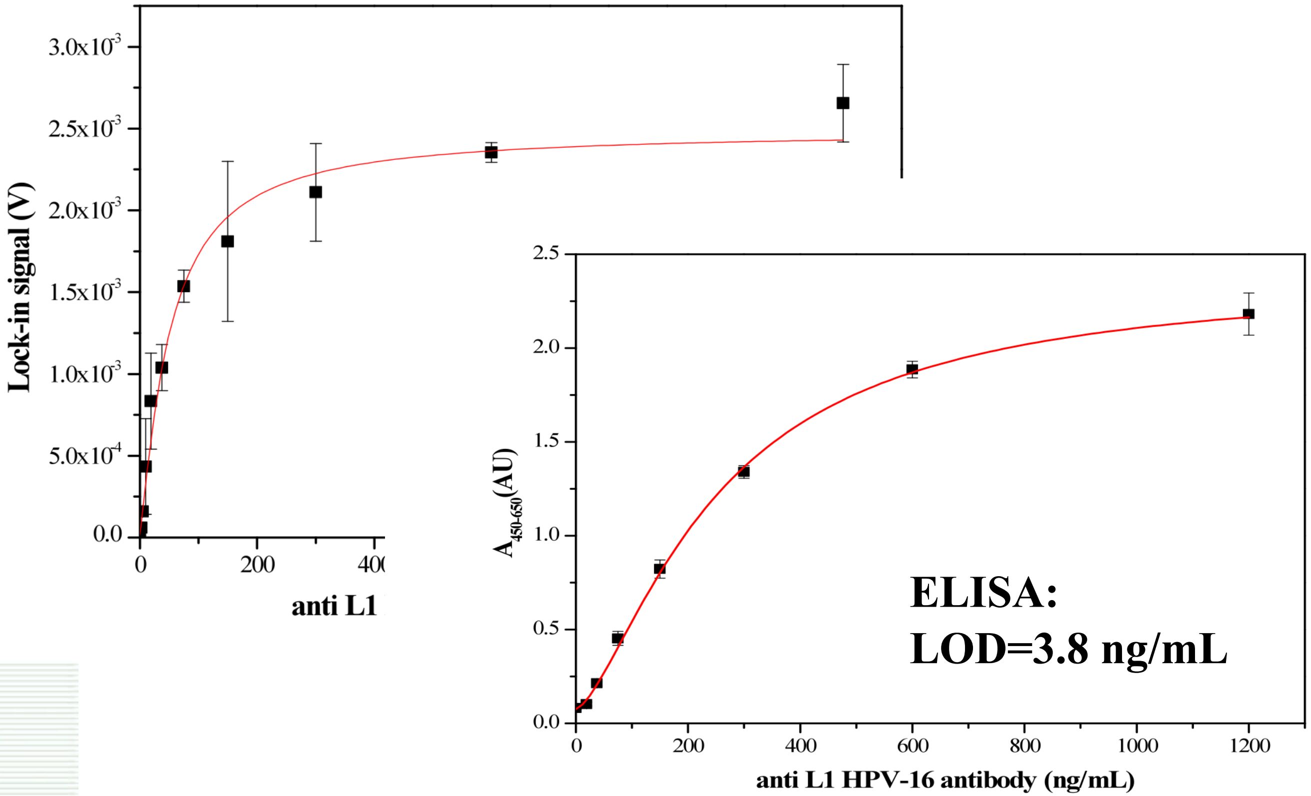

Sample	*ELISA (ng/mL)*	*Microtiter μFIA-TLM (ng/mL)*	*Nanobeads μFIA-TLM (ng/mL)*
1	6.9 ± 0.1	7 ± 1	6.8 ± 0.9
2	8.2 ± 0.8	7.3 ± 0.2	8 ± 1
3	5.9 ± 0.5	5.2 ± 0.8	5.4 ± 0.2
4	below LOD	3.0 ± 0.4	3.8 ± 0.6

First detection and modulation of bilirubin in vascular endothelial cels

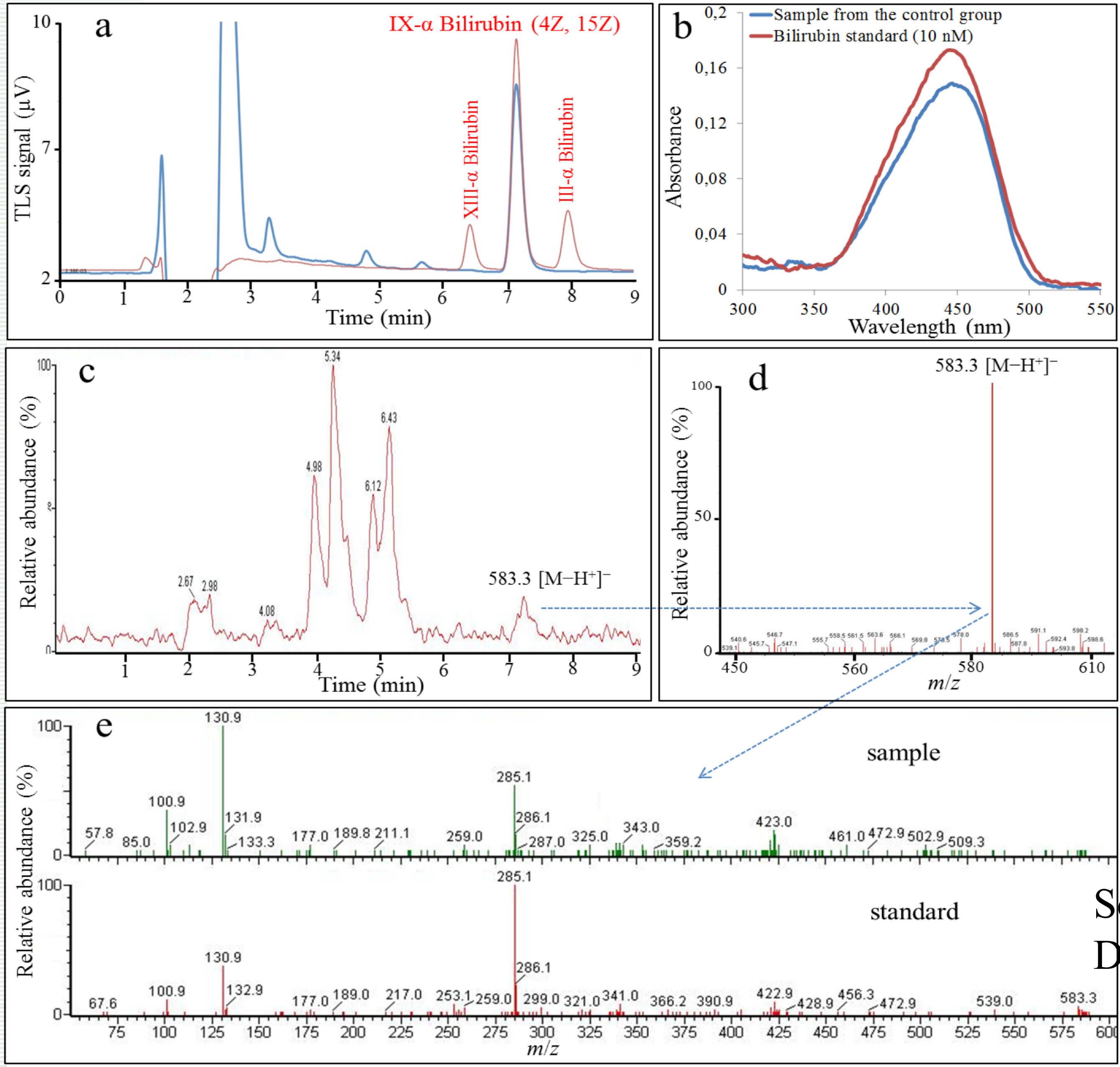

Rat aortha/vein endothelium:
1.53 ± 0,57 / 0.93 ± 0,14 pmol BR/mg protein

LOQ for HPLC-TLS:
0.12 pmol/mg protein

Scientific Reports 6:29240
DOI: 10.1038/srep29240

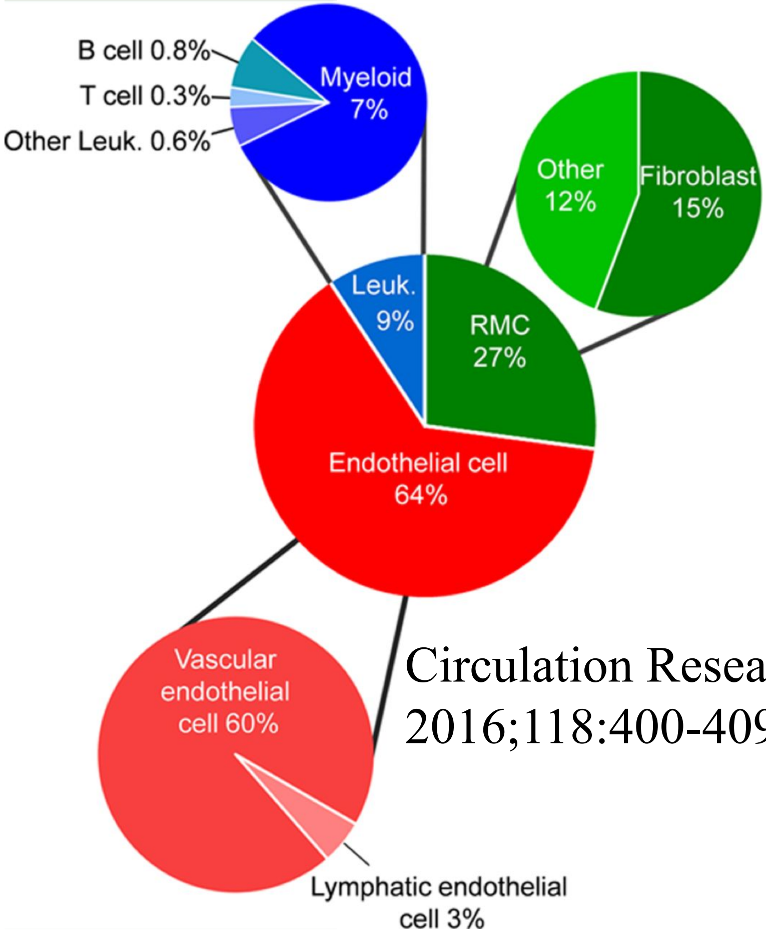

Circulation Research. 2016;118:400-409

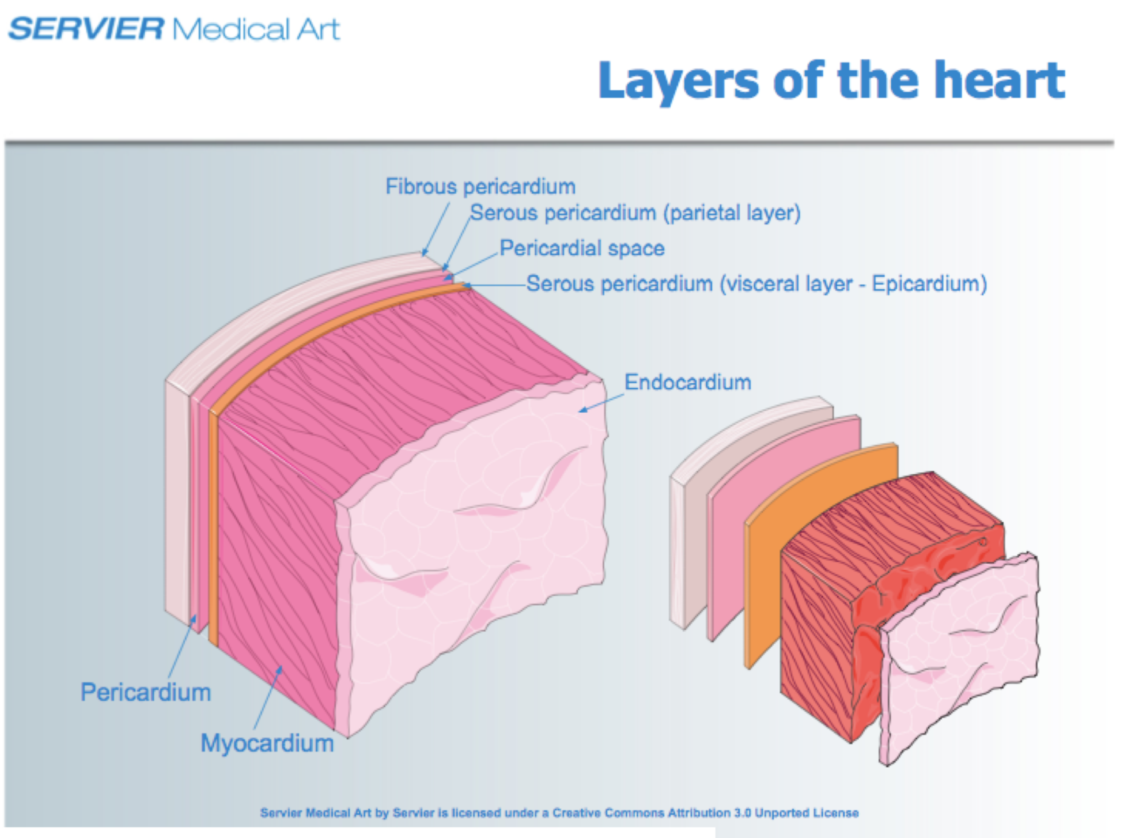

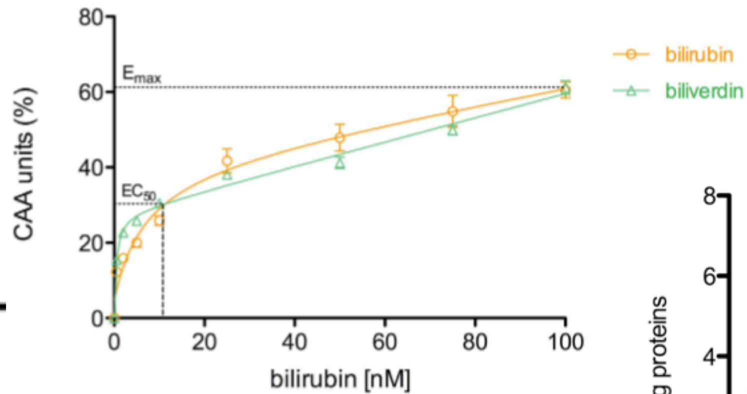

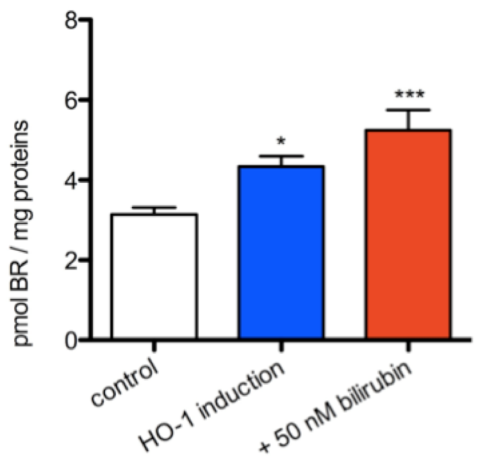

SCIENTIFIC REPORTS

OPEN

Bilirubin is an Endogenous Antioxidant in Human Vascular Endothelial Cells

Received: 29 December 2015
Accepted: 14 June 2016

Lovro Ziberna[1,2], Mitja Martelanc[3], Mladen Franko[3] & Sabina Passamonti[3]

Acknowledgements

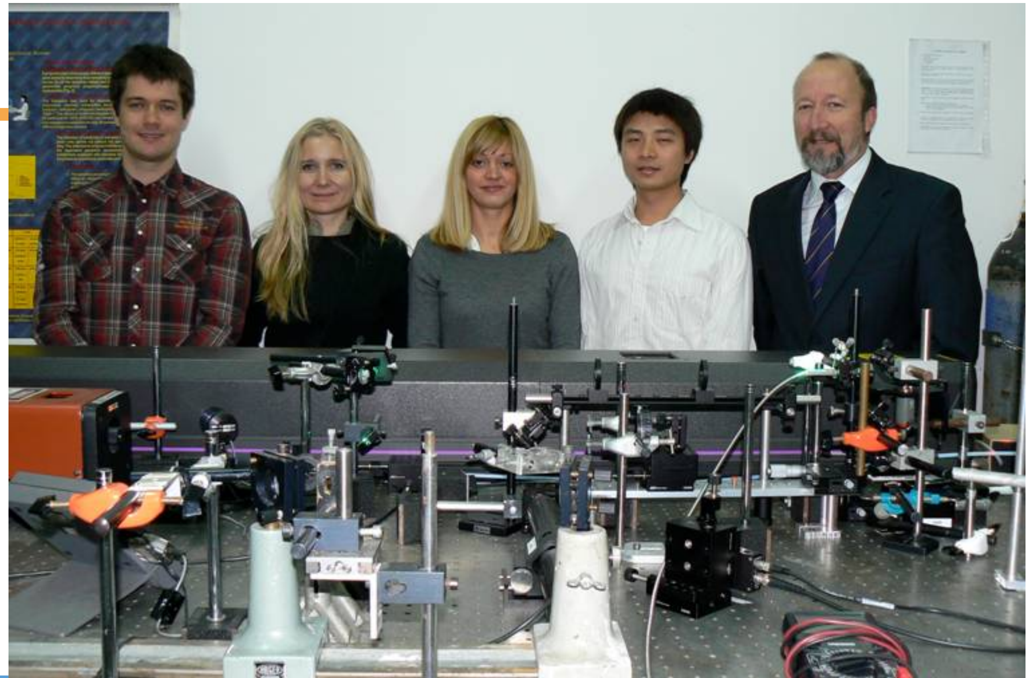

- Dorota Korte
- Mitja Martelanc
- Mingqiang Liu
- Tatjana Radovanović
-Vukajlović
- Lea Goljat

- Funding: ARRS,

- Humberto Cabrera
- Lovro Žiberna
- Sabina Passamonti
- Matjaž Klemenc

Basic literature on TLS

- S.E. Bialkowski, *Photothermal Spectroscopy Methods for Chemical Analysis*, John Whiley & Sons, Inc., New York, 1996.
- C.D. Tran , M. Franko, "*Thermal Lens Spectroscopy*" in: Encyclopedia of Analytical Chemistry, (Ed. R.A. Meyers), John Wiley: Chichester., 2010. DOI: 9780470027318.
- M. Franko*, "Bioanalytical Applications of TLS"*, in: Thermal wave physics and related photothermal techniques: Basic principles and recent developments, ISBN 978-81-7895-401-1 (Ed. E. Marin), Research Signpost Press, 2009
- M. Franko, Thermal Lens Spectrometric Detection in Flow Injection Analysis and Separation Techniques, *Appl. Spectrosc. Rev*. **43**, 2008, 358-388.

Basic literature on TLS

- Kitamori, T., Tokeshi, M., Hibara, A. and Sato, K., Thermal lens microscopy and microchip chemistry. *Anal. Chem.*, **76**, 2004, 52A-60A.
- M. Franko, C.D. Tran, Analytical Thermal Lens Instrumentation, *Rev. Sci. Instrum*. **67**, 1996, 1-18.
- Liu M., Franko M.: Progress in thermal lens spectrometry and its application in microscale analytical devices, *Crit. Rev. Anal. Chem.* **44**, 2014, 328-353.